Atmospheric Solar Heating in Minor Absorption Bands

Ming-Dah Chou
Laboratory for Atmospheres
NASA/Goddard Space Flight Center
Greenbelt, Maryland
USA

November, 1998
Terrestrial, Atmospheric and Oceanic Sciences

Corresponding author: Dr. Ming-Dah Chou
Code 913
Laboratory for Atmospheres
NASA/Goddard Space Flight Center
Greenbelt, MD 20771
Telephone: 301-286-4012
FAX: 301-286-1759
e-mail chou@climate.gsfc.nasa.gov

ABSTRACT

Solar radiation is the primary source of energy driving atmospheric and oceanic circulations. Concerned with the huge computing time required for computing radiative transfer in weather and climate models, solar heating in minor absorption bands has often been neglected. The individual contributions of these minor bands to the atmospheric heating is small, but collectively they are not negligible. The solar heating in minor bands includes the absorption due to water vapor in the photosynthetically active radiation (PAR) spectral region from 14284 cm^{-1} to 25000 cm^{-1}, the ozone absorption and Rayleigh scattering in the near infrared, as well as the O_2 and CO_2 absorption in a number of weak bands. Detailed high spectral- and angular-resolution calculations show that the total effect of these minor absorption is to enhance the atmospheric solar heating by ~10%. Depending upon the strength of the absorption and the overlapping among gaseous absorption, different approaches are applied to parameterize these minor absorption. The parameterizations are accurate and require little extra time for computing radiative fluxes. They have been efficiently implemented in the various atmospheric models at NASA/Goddard Space Flight Center, including cloud ensemble, mesoscale, and climate models.

1. INTRODUCTION

The ultimate force driving the Earth's weather and climate is the solar radiation. Satellite measurements of the earth radiation budgets show that the Earth reflects ~30% of the incoming solar radiation, and the rest is absorbed at the surface and in the atmosphere (Barkstrom, 1984, Kandel et al., 1998). Partitioning of the 70% of the solar heating between the surface and the atmosphere is very important to oceanic and atmospheric circulations; a larger solar heating at the surface will cause a higher surface temperature and an enhanced evaporation, leading to a more energetic atmospheric circulation. However, this partitioning cannot be directly estimated from currently available satellite measurements. It can only be estimated either from model calculations or from surface measurements with accuracies not well known. The Atmospheric Radiation Measurements (ARM) program of the US Department of Energy has conducted a number of field experiments to study the radiative processes in the atmosphere. Both narrow- and broad-band flux measurements are compared with theoretical model calculations. The aim is to provide information for validating radiation parameterizations used in numerical weather and climate models. It is clear that accurate calculations of solar heating is important in climate studies using computer models.

The broadband parameterizations for solar radiation used in weather and climate studies are mostly based on high spectral resolution calculations of gaseous absorption and detailed angular integration of particle scattering. To enhance computing speed, the spectrum is divided into a small number of bands, and only important gaseous absorption and particle scattering are included. Minor absorption and scattering due to gases or scatterers spread over a wide spectral range. They are almost always neglected in radiation models used in weather and climate studies in order to save computing time. Individua y their effects are small, but the total effect may not be negligible. As the capability of the computing system increases, more detailed physical processes are included and higher spatial and temporal resolutions are used in weather and climate models. To be consist with these improvements, radiative transfer calculations are required to be more accurate than the existing models. Because calculations of radiative terms in weather and climate models require a large portion of the total computing time, it is essential that improvement in radiation parameterization should not have a large impact on computing speed.

There are a number of solar radiation schemes available for use in global climate models (cf. Fouquart et al., 1991). At NASA/Goddard Space Flight Center, a series of parameterizations for radiative transfer in the solar spectrum due to various absorbers and scatterers has been developed and applied to global and regional climate studies (Chou, 1986; Chou, 1992; Chou and Lee, 1996). The ozone absorption and Rayleigh scattering were included in the ultraviolet (UV) and visible regions with the wavenumber $\nu > 14285$ cm^{-1} (0.7 μm) but were neglected in the near infrared. On the other hand, the absorption due to water vapor was included in the infrared with $\nu < 14285$ cm^{-1} but were neglected in the photosynthetically active radiation (PAR) region between 14285 cm^{-1} and 25000 cm^{-1}. (0.4 μm and 0.7 μm). Oxygen and CO_2 also absorb solar radiation in the infrared. The parameterizations only included the absorption in major O_2 and CO_2 bands. Absorption in minor O_2 and CO_2 bands, which scatter over wide spectral ranges, was neglected. Individually, these weak absorption and scattering neglected in the parameterizations have a little effect on solar heating of the atmosphere. Collectively, their effect is not necessarily negligible. This study presents the parameterizations for the minor absorption and scattering, which have been efficiently implemented into the mesoscale and global atmospheric models used at NASA/Goddard Space Flight Center.

2. MINOR GASEOUS ABSORPTION AND RAYLEIGH SCATTERING

In a clear atmosphere, the heating of the atmosphere is primarily due to water vapor and O_3 and secondarily due to O_2 and CO_2. Rayleigh scattering interacts with absorption and affects solar heating in the atmosphere and at the surface. Both the ozone absorption coefficient and the Rayleigh scattering coefficient decrease rapidly with decreasing wavenumber ν. Figure 1 shows the spectral distribution of the ozone transmission function of the entire atmospheric column in the vertical direction. The Rayleigh scattering (not shown in the figure) decreases with decreasing wavenumber according to ν^4. For $\nu<14285$ cm^{-1}, the ozone absorption and Rayleigh scattering are both weak and were not included in the radiation model. Water vapor absorbs solar radiation at all wavelength except in the UV region. Figure 2 shows the spectral distribution of the water vapor transmission function of the atmosphere in the vertical direction. The width of water vapor molecular lines is small compared to the mean line spacing. As a result, the absorption coefficient varies rapidly within a narrow spectral interval. The transmission function shown in Fig. 2 is the mean over 10 cm^{-1}. It can be seen that there are many water vapor absorption bands with band-strength decreases rapidly with increasing ν. The bands in the high frequency region with $\nu>14285$ cm^{-1} are very weak and were neglected in our radiation model.

In addition to water vapor and O_3, oxygen and CO_2 also absorb solar radiation. Figures 3 and 4 show, respectively, the spectral distributions of the O_2 and CO_2 transmission functions of the entire atmospheric column. The two major O_2 A and B bands are located at 13150 cm^{-1} and 14550 cm^{-1}. There are also minor bands located at 7890 cm^{-1} and 15870 cm^{-1}. Only the two major A and B bands were included in our radiation model. Carbon dioxide absorbs solar radiation in a wide spectral range. Only the absorption in 3600 cm^{-1} and 5000 cm^{-1} bands were included. The absorption in the 2325 cm^{-1} (4.3 μm) band is very strong, but the insolation (incoming solar radiation) is small. Solar heating due to CO_2 in this band is small and was not included in the radiation model. There is also absorption due to CO_2 in the spectral region between 6000 cm^{-1} and 7000 cm^{-1} (1.43 μm and 1.67 μm). The solar energy contained in this spectral regions is large, but the absorption coefficient is small. It was also not included in the radiation model. Table 1 shows the major absorption and scattering included in our radiation model, and Table 2 shows those minor absorption and scattering which were not included in the radiation model but are parameterized in this study.

3. HIGH SPECTRAL-RESOLUTION CALCULATIONS

Parameterizations for solar fluxes in minor absorption bands are based on high spectral- and angular-resolution calculations. The temperature, humidity, and ozone profiles are typical of a mid-latitude summer atmosphere taken from Anderson et al., (1986), which has a vertically integrated water vapor amount of 2.93 g cm^{-2} and ozone amount of 0.318 $(cm\text{-}atm)_{STP}$. The CO_2 concentration is set to be 350 ppmv at all heights, and the O_2 mass mixing ratio is fixed at 0.2315.

The O_3 absorption coefficient varies by several orders of magnitude in the UV and visible regions but rather smoothly with wavenumbers. Fluxes are computed with a spectral resolution of 1 cm^{-1} with the O_3 absorption coefficient interpolated from the spectral values given in WMO (1985). The absorption coefficients of water vapor, O_2 and CO_2 vary rapidly with wavenumber, and the line-by-line method is used to compute the absorption coefficients. The 1996-version of the molecular line parameters compiled at AFGL (Rothman, 1987) are used in the line-by-line calculations. The shape of an absorption line is assumed to follow the Voigt function. Because the shape of the far wings of a line is not well known, the absorption coefficient is set to zero at wavenumber >10 cm^{-1} from the line center. The spectral resolution of the line-by-line calculations is chosen to be 0.005 cm^{-1}, which is adequate for flux calculations in the troposphere. Rayleigh scattering is computed using the discrete-ordinate multiple-scattering algorithm of Stamnes, et al. (1988). The number of angular streams used is six. The spectral resolution used in computing Rayleigh scattering is either 1 cm^{-1} when overlapping with the O_3 absorption or 0.005 cm^{-1} when overlapping with the water vapor absorption.

4. BROADBAND TRANSMISSION AND FLUX PARAMETERIZATIONS

4.1 The k-distribution method

The width of an absorption line of water vapor, O_2, and CO_2 is much smaller than the average spacing between absorption lines. The width of a line decreases linearly with pressure and is only ~0.05 cm^{-1} in the lower troposphere. As a result, the absorption coefficient varies very rapidly within narrow spectral intervals, and accurate radiative transfer calculations require a high spectral resolution. For the case of water vapor absorption, the high resolution line-by-line method requires flux calculations at $>10^6$ spectral points. For an atmospheric layer where temperature and pressure can be assumed constant, the wavenumbers with the same absorption coefficient are radiatively identical and can be treated as one entity. Fluxes at those wavenumbers with the same absorption coefficient need to be computed only once. Therefore, flux calculations can be greatly simplified by grouping the wavenumbers with the same absorption coefficient. Within a small interval $\Delta\nu$ where the spectral variation of insolation is small, the integration of fluxes over wavenumbers can be replaced by that over the absorption coefficient. The mean transmission function of the interval $\Delta\nu$ can be written as

$$\tau(w') = \int_{\Delta\nu} e^{-k_\nu w'} d\nu / \Delta\nu = \int_0^\infty e^{-kw'} g(k) dk \approx \sum_{i=1}^{n} a_i e^{-k_i w'} \qquad (1)$$

where w' is the absorber amount, k_ν is the absorption coefficient at the wavenumber ν, g is the k-distribution density function (cf. Arking and Grossman, 1972) such that the fraction of spectrum with the absorption coefficient in the between $k-\frac{1}{2}dk$ and $k+\frac{1}{2}dk$ is $g(k)dk$, and a_i $(=g(k_i)\Delta k_i)$ is the k-distribution function. It has been found (Chou and Lee, 1996) that the k-distribution method requires only ~10 values of k (i.e. n~10) for accurate calculations of solar fluxes using the k-distribution method instead of $>10^6$ spectral points using the line-by-line method.

In the atmosphere where pressure and temperature change with height, the wavenumbers with a common absorption coefficient at a given height will not necessarily have a common absorption coefficient at other heights. These wavenumbers are no longer radiatively identical, and the k-distribution method cannot be used without applying assumptions. Pressure affects the width of an absorption line. Near the center of a line, the absorption is strong, and flux calculations are not sensitive to errors in the absorption coefficient. Distant from line centers, the absorption coefficient increases nearly linearly with pressure. On the other hand, temperature affects absorption primarily through its effect on the line intensity, which is constant for a given line. Thus, the temperature effect on absorption is rather smooth with respect to wavenumber. It has been shown by Chou (1986) that fluxes can be calculated accurately with the use of the one-parameter scaling of the absorption coefficient,

$$k_\nu(p,T) = k_\nu(p_r,T_r)\left(\frac{p}{p_r}\right)^m f(T,T_r) \qquad (2)$$

where p_r is the reference pressure, T_r is the reference temperature, $m \leq 1$, and $f(T,T_r)$ is the temperature scaling function. As explained in Chou (1986), the optical path between the top of the atmosphere and the middle and lower troposphere is long near the center of absorption lines. Solar fluxes in middle and lower troposphere are primarily attributable to the spectral intervals between absorption lines, and the wing-approximation of (2) can be applied to accurately compute fluxes. In the stratosphere, the solar heating due to water vapor, O_2, and CO_2 is small, and underestimation of the absorption coefficient induced by the use of (2) does not have a significant effect on the heating rate. In the upper troposphere, the absorption is neither strong nor weak, and the error induced by the scaling is expected to have a large impact on flux calculations. However, if we choose p_r to be the upper troposphere pressure, then $p / p_r \approx 1$ in the upper troposphere, and the scaling introduces only a small error in the absorption coefficient. It has been found (Chou, 1986) that the solar fluxes can be computed accurately by choosing p_r=300 hPa and m=0.8. Flux calculations are not sensitivity to m for 0.7< m<0.9. The effect of temperature on the absorption of solar radiation is weak. For the absorption due to water vapor, the temperature effect on absorption is approximated by using

$$f(T,T_r) = 1 + 0.00135(T - T_r) \tag{3}$$

where T_r=240 K. For the absorption due to O_2, and CO_2, the temperature effect is neglected, i.e. $f(T,T_r)=1$.

Using the scaling of (2), Equation (1) becomes

$$\tau(w) = \sum_{i=1}^{n} a_i e^{-k_i(p_r,T_r)w} \tag{4}$$

where

$$w(p,T) = w'\left(\frac{p}{p_r}\right)^m f(T,T_r) \tag{5}$$

Thus, the scaling of the absorption coefficient is reduced to the scaling of the absorber amount, and flux calculations are greatly simplified. It is noted that the basis for the k-distribution method with the one-parameter pressure and temperature scaling is the same as the correlated k-distribution method (Goody et al., 1989; Lacis and Oinas, 1991; Fu and Liou, 1992), i.e. the dominant effect of line wings on the absorption. The accuracies of these two approaches are comparable, but the former is much simpler than the latter.

4.2 <u>Flux calculations</u>

For a spectral band with a width $\Delta\nu$, the direct solar flux at a given pressure level p can be written as

$$F(w) = \int_{\Delta\nu} e^{-k_\nu w} S_\nu d\nu \tag{6}$$

where S_ν is the extraterrestrial solar flux density at the wavenumber ν multiplied by the cosine of the solar zenith angle, k is the absorption coefficient, and w is the scaled absorber amount above the pressure level p in the direction of the solar beam. The mean transmission of a band is given by

$$\tau(w) = \int_{\Delta\nu} e^{-k_\nu w} S_\nu d\nu \Big/ \int_{\Delta\nu} S_\nu d\nu \tag{7}$$

If we divide a spectral band into m small intervals and apply the k-distribution method, Equation (6) becomes

$$F(w) = \sum_{j=1}^{m} S_j \left[\int_{\Delta\nu_j} e^{-k_\nu w} d\nu \right] = \sum_{i=1}^{n} \left[\sum_{j=1}^{m} a_{i,j} S_j \Delta\nu_j \right] e^{-k_i w} \tag{8}$$

where S_j is the mean flux density in the interval $\Delta\nu_j$, $a_{i,j}$ is the k-distribution function in the interval $\Delta\nu_j$, n is the number of the absorption coefficient k, and

$$\Delta\nu = \sum_{j=1}^{m} \Delta\nu_j \tag{9}$$

By defining

$$S = \sum_{j=1}^{m} S_j \Delta\nu_j \tag{10}$$

and

$$h_i = \sum_{j=1}^{m} a_{i,j} S_j \Delta\nu_j / S \tag{11}$$

Equation (8) becomes

$$F(w) = S\tau(w) \tag{12}$$

where $\tau(w)$ is the mean transmission function of the band $\Delta\nu$ given by

$$\tau(w) = \sum_{i=1}^{n} h_i e^{-k_i w} \tag{13}$$

and h_i is the flux-weighted k-distribution function at p_r=300 hPa and T_r=240 K which has the property

$$\sum_{i=1}^{n} h_i = 1 \tag{14}$$

To simplify flux calculations involving scattering, a single value of the scattering coefficient is used for each band. Because scattering of light varies slowly with wavenumber, this approximation will not introduce large errors in flux calculations. Using the k-distribution method for absorption and the δ-Eddington approximation (Joseph et al., 1976) for scattering, transmission and reflection functions of each layer are first computed for each value of k. The two -stream adding method (cf. Chou, 1992) is then used to compute the fluxes components F_i associated with k_i, i=1, 2, ... , n. The total flux of a band is the sum of F_i weighted by the k-distribution function,

$$F(w) = \sum_{i=1}^{n} h_i F_i(w) \tag{15}$$

This approach is applied to computing fluxes due to water vapor absorption in the infrared.

For the case that either the range of k or the value of k itself is small within a spectral band, the transmission can be approximated by

$$\tau(w) = e^{-\bar{k}w} \tag{16}$$

where $\bar{k}$ is the mean absorption coefficient of a spectral band. This approach is applied to computing fluxes due to O_3 absorption.

Absorption due to O_2 and CO_2 are treated differently from the absorption due to water vapor and O_3. The major absorption due to O_2 is not weak but occurs in narrow spectral intervals. An effective absorption coefficient of O_2 is derived by fitting the mean transmission function $\tau(w)$ computed from the line-by line method,

$$\tau(w) = e^{-\bar{k}\sqrt{w}} \tag{17}$$

The O_2 absorption bands are located between water vapor absorption bands. Thus, water vapor has little effect on the solar heating due to O_2. Instead of computing fluxes in the O_2 bands, the reduction in fluxes due to O_2 absorption is computed from

$$\Delta F(w) = S\left(1 - e^{-\bar{k}\sqrt{w}}\right) \tag{18}$$

Here S is the insolation at the top of the atmosphere in the O_2 bands. Because scattering algorithms are developed for monochromatic radiation, the band-averaged transmittance (17) can only be applied to clear-skies but not to cloudy skies.

The absorption due to CO_2 is small but overlaps significantly with the absorption due to water vapor. Similar to (6) and (12), fluxes in the CO_2 bands are given

$$F(w,u) = \int e^{-(k_\nu w + \gamma_\nu u)} S_\nu d\nu = S\tau(w,u) \tag{19}$$

where w and u are the scaled water vapor and CO_2 amounts, k and γ are the absorption coefficients of water vapor and CO_2, $\tau(w,u)$ is the transmittance defined by

$$\tau(w,u) = \sum_{i=1}^{n}\sum_{j=1}^{m} h_{i,j} e^{-(k_i w + \gamma_j u)} \tag{20}$$

and $h_{i,j}$ is the flux-weighted k-distribution function with the absorption coefficients k_i and γ_j for the two absorbers, respectively. Equation (20) requires (m x n) sets of flux calculations, which becomes computationally very expensive when used in weather and climate models. Other approaches than the k-distribution method have to be used for efficient flux calculations when overlapping of absorption is involved.

The flux-weighted transmittance involving two absorbers can be pre-computed as a function of w and u, and fluxes can be computed from (19), or alternatively from

$$F(w,u) = F(w) - \Delta F(w,u) \tag{21}$$

where $\Delta F(w,u)$ is the flux reduction due to CO_2 with amount u,

$$\Delta F(w,u) = \int e^{-k_\nu w}\left(1 - e^{-\gamma_\nu u}\right) S_\nu d\nu \tag{22}$$

and the integration is over the entire solar spectrum. A two-dimensional table for $\Delta F(w,u)$ is pre-computed using the line-by-line method.

Table 1 shows the spectral bands of the solar radiation model used at NASA/Goddard Space Flight Center. There are eight bands in the ultraviolet and visible region (ν>14285 cm^{-1}) and three bands in the infrared region (ν<14285 cm^{-1}). Also shown in the table are the absorbers and scatterers included in the calculation of solar fluxes in each band, as well as the equations used for computing the transmission function. The first eight bands involves the ozone absorption and Rayleigh scattering. These bands are narrow, and an effective ozone absorption coefficient and an effective Rayleigh scattering coefficient are used for each band. The effective Rayleigh scattering coefficient is derived by averaging the flux-weighted scattering coefficient over a band. For the ozone absorption, we first compute $\tau(w)$ from (7) with a high spectral resolution. The effective absorption coefficient, $\bar{k}$, is then derived by fitting $\tau(w)$ with (16). The absorption due to water vapor is included in the three infrared bands (Bands 9, 10, and 11). The water vapor absorption varies strongly within small spectral intervals, and the k-distribution function method, Equations (13) and (15), is used to compute fluxes. The number of the absorption coefficient used in each band is 10. The use of this number is to avoid oscillation in the vertical profile of the computed heating rate when a smaller number is used (Chou and Lee, 1996). The absorption due to O_2 and CO_2 occur in wide spectral ranges. The flux reduction due to O_2 is computed from (17) and that due to CO_2 is computed from $\Delta F(w,u)$ using table look-up. Because clouds have a large impact on radiation, we can neglect the weak absorption due to O_2 and CO_2 within clouds. The flux reduction ΔF is computed only for clear skies or the level above the cloud top. Below the cloud top, it is set to that at the cloud top.

5. ABSORPTION IN MINOR BANDS

5.1 Water vapor absorption in $\nu \geq 14285$ cm^{-1}

The absorption due to water vapor in the photosynthetically active radiation (PAR) region between 14285 cm^{-1} and 22700 cm^{-1} (0.7 μm and 0.44 μm) was not included in

Band 8 of our radiation model. Because the absorption due to water vapor is weak in this spectral region, it can be represented by a single effective absorption coefficient $\bar{k}$ in (16). To derive $\bar{k}$, the mean transmission function $\tau(w)$ given by (7) is first computed using the line-by-line method for w ranging from 5 g cm^{-2} to 20 g cm^{-2}. For each w, an effective absorption coefficient is computed from

$$\bar{k}(w) = -\frac{1}{w} \ln \tau(w) \tag{23}$$

The value of $\bar{k}$ at p_r=300 hPa and T_r=240 K is found to range from 0.00065 to 0.00080 g^{-1} cm^2, and a mean value of 0.00075 g^{-1} cm^2 is adopted in the broadband flux calculations. For the midlatitude summer atmosphere, the vertical-integrated scaled water vapor amount in the direction 60° from the zenith is 14 g cm^{-2}, and the absorptance in the PAR spectral region is ~0.01. With a fraction of 0.391 of the extraterrestrial solar radiation contained in the PAR, it corresponds to an atmosphere solar heating of ~2.6 W m^{-2}. Table 3 shows that the surface flux reduction in Band 8 due to water vapor is 2.53 W m^{-2} from line-by-line calculations and 2.42 W m^{-2} from the parameterization. Rayleigh scattering and O_3 absorption have little effect on the absorption due to water vapor in the PAR.

5.2 Ozone absorption in $\nu \leq 14285$ cm^{-1}

As shown in Figure 1, the absorption due to ozone in the near infrared (Band 9) is restricted to a narrow spectral region next to Band 8 where absorption due to water vapor is weak. However, the absorption due to water vapor in the rest of Band 9 is not necessarily weak, and calculations of ozone heating in the near infrared would require adding another band in the broadband radiation model. Because the absorption due to water vapor and O_3 is weak in Band 8, the O_3 absorption in Band 9 can be folded into the absorption in Band 8 as if it were the absorption due to another absorber. To do so, the effective O_3 absorption coefficient of Band 8 is enhanced by Δk which satisfies

$$\left(1-e^{-\Delta k w'}\right)\int_{\Delta\nu_1} S_\nu d\nu = \int_{\Delta\nu_2}\left(1-e^{-k_\nu w'}\right) S_\nu d\nu \qquad (24)$$

so that the absorption of solar radiation due to O_3 in the near infrared is correctly computed, where w' is the ozone amount, and $\Delta\nu_1$ and $\Delta\nu_2$ are the widths of Bands 8 and 9, respectively. It is noted that the absorption due to ozone is nearly independent of pressure and temperature, it is not necessary to scale the ozone amount given by (5). For a wide range of w' found in the atmosphere, the value of Δk ranges between 0.0032 and 0.0033 $(\text{cm-atm})_{STP}^{-1}$. Therefore, the ozone absorption coefficient in Band 8 is enhanced by 0.0033 $(\text{cm-atm})_{STP}^{-1}$ to take into account the absorption by ozone in the infrared. This approach to computing the ozone absorption in the near infrared requires no extra computing time. For the midlatitude summer atmosphere, the column ozone amount is 0.318 $(\text{cm-atm})_{STP}$. It can be easily shown that the solar heating of the atmospheric column is enhanced by 0.56 W m^{-2}, which is independent of the solar zenith angle due to the opposite impacts of the solar zenith angle on the insolation and the ozone pathlength. Table 3 shows that the surface flux reduction in the near infrared due to O_3 is 0.54 W m^{-2} as computed from the parameterization, which is very close to that computed with a high spectral resolution.

5.3 Oxygen absorption

As shown in Figure 3, the absorption due to O_2 occurs in narrow spectral intervals, but is not necessary weak near band centers. In the parameterization of the O_2 absorption, Chou (1990) computed the mean transmission function in the O_2 A and B bands centered at 13150 cm^{-1} and 14510 cm^{-1} and fit the transmission function by (17). The absorption in the weak bands centered at 7890 cm^{-1} and 15870 cm^{-1} was not included. Line-by-line calculations show that the total atmospheric heating due to O_2 is 4.29 W m^{-2} for a solar zenith angle of 60°. The O_2 A and B bands contribute 3.70 W m^{-2} to the total absorption. A heating of 0.49 W m^{-2} is attributable to the band 7700-8050 cm^{-1} and 0.1 W m^{-2} is attributable to the band 15750-15950 cm^{-1}. Thus, excluding the two weak bands will cause an underestimation of the atmospheric heating by 0.50 W m^{-2}.

To include the absorption in all those bands, the mean transmission function of O_2 at p_r=300 hPa and T_r=240 K in the spectral regions 7600-8050, 12850-13190, 14310-14590, and 15730-15930 cm^{-1} is computed from (7) using the line-by-line method, and the effective mean absorption coefficient $\bar{k}$ is computed from

$$\bar{k}(w) = -\frac{1}{\sqrt{w}} \ln \tau(w) \tag{25}$$

The value of $\bar{k}$ is between 0.000135 $(\text{cm-atm})_{STP}^{-1/2}$ and 0.000155 $(\text{cm-atm})_{STP}^{-1/2}$ for a large range of w encountered in the atmosphere, and a mean value of 0.000145 $(\text{cm-atm})_{STP}^{-1/2}$ is adopted to compute the flux reduction due to O_2 from (18). The insolation, S, in the spectral regions 7600-8050, 12850-13190, 14310-14590, and 15730-15930 cm^{-1} is 86.53 W m^{-2} or 6.33% of the total solar flux at the top of the atmosphere. Table 3 shows that, for a solar zenith angle of 60°, the surface flux reduction due to O_2 is 4.29 W m^{-2} from line-by-line calculations and 4.18 W m^{-2} from the parameterization.

5.4 Carbon dioxide absorption

The absorption of solar radiation due to CO_2 spreads over the middle infrared from 2000 to 7000 cm^{-1}. It overlaps substantially with the absorption due to water vapor in some spectral regions. Line-by line calculations show that, for a solar zenith angle of 60° and a CO_2 concentration of 350 ppmv, the atmosphere heating due to CO_2 alone is 8.73 W m^{-2} but reduces to 3.30 W m^{-2} when overlaps with water vapor absorption in the mid-latitude summer atmosphere. Because of this strong overlapping, the CO_2 transmission function cannot be computed independently of water vapor.

From the pre-computed table of $\Delta F(w,u)$ given by (22), Chou (1990) compute the flux reduction due to CO_2 only for the spectral bands centered at ~3700 cm^{-1} and 5000 cm^{-1}. To include the CO_2 absorption in the minor bands, the flux reduction $\Delta F(w,u)$ is re-computed in this study to cover the entire solar spectrum which includes the strong b

2480 cm^{-1} and the weak bands at 6300 cm^{-1} and 7000 cm^{-1}. Line-by-line calculations show that, for the mid-latitude summer atmosphere, a solar zenith angle of 60°, and a CO_2 concentration of 350 ppmv, the surface flux reduction due to CO_2 increases by 1.21 W m^{-2} when the minor absorption is included. Table 3 shows that the flux reduction computed from the parameterization is 3.60 W m^{-2} which is slightly larger than that from line-by-line calculations.

5.5 Rayleigh scattering in the near infrared

Rayleigh scattering in the near infrared is weak and was neglected in our radiation model. To include the Rayleigh scattering in the near infrared, a mean extinction coefficient for each of two near infrared bands, Bands 9 and 10, is computed from

$$\bar{\sigma} = \int \sigma_v S_v dv \,/ \int S_v dv \qquad (26)$$

where the integration is over the spectral interval of a band. The value of $\bar{\sigma}$ is 0.0000156 hPa^{-1} for Band 9 and 0.0000017 hPa^{-1} for Band 10. Rayleigh scattering in Band 11 is negligible. The effect of Rayleigh scattering in the midlatitude summer atmosphere with a solar zenith angle of 60° and a surface albedo of zero is shown in Table 3. Rayleigh scattering reduces the surface radiation by 3.12 W m^{-2} from the line-by-line and discrete-ordinate calculations and by 2.82 W m^{-2} using a mean extinction coefficient.

6. CONCLUSIONS

Calculations of radiative heating/cooling in the atmosphere require a large portion of the total computing time in global climate simulations using a general circulation model. To enhance the efficiency of radiation calculations, much of the atmospheric solar heating in minor bands are neglected. Individually, these minor heating terms are small, but collectively they are not negligible. It is found from high spectral- and angular-resolution calculations that the absorption due to water vapor in the photosynthetically active radiation (PAR) band and that due to CO_2 in middle infrared amount to ~5.5 W m^{-2} for a midlatitude summer atmosphere and a solar zenith angle of 60°. The absorption due to O_2 and O_3 in the near infrared amount to ~5.0 W m^{-2}. Raleigh scattering in the near infrared reduces the surface solar heating by ~3 W m^{-2}. The sum of these heating is ~10% of the total solar heating of the Earth's surface, which is not negligible. In this study, different parameterizations are applied to these minor absorption and scattering depending upon the strength of the extinction and the overlapping of absorption among various absorbers. The parameterizations are accurate and require little extra computing time. Therefore, they are suitable for climate studies using an atmospheric general circulation model.

Acknowledgments This study was supported by the Global Atmospheric Modeling and Analysis Program, NASA/Office of Earth Science.

REFERENCES

Anderson, G. P., S. A. Clough, F. X. Kneizys, J. H. Chetwynd, and E. P. Shuttle, 1986: AFGL atmospheric constituent profiles (0-120 km), AFGL-TR-86-0110, 43 pp. [NTIS ADA175173]

Arking, A., and K. Grossman, 1972: The influence of line shape and band structure on temperatures in planetary atmospheres. *J. Atmos. Sci.*, **29**, 937-949.

Barkstrom, B. R., 1984: The Earth Radiation Budget Experiment (ERBE). *Bull. Amer. Meteorol. Soc.*, **65**, 1170-1185.

Chou, M.-D., 1986: Atmospheric solar heating rate in the water vapor bands. *J Climate Appl. Meteor.*, **25**, 1532-1542.

Chou, M.-D., 1992: A solar radiation model for use in climate studies. *J. Atmos. Sci.,* **49**, 762-772.

Chou, M.-D., and K.-T. Lee, 1996: Parameterizations for the absorption of solar radiation by water vapor and ozone. *J. Atmos. Sci*, **53**, 1203-1208.

Fu, Q, and K.-N. Liou, 1992: On the correlated k-distribution method for radiative transfer in nonhomogeneous atmospheres. *J. Atmos. Sci.*, **49**, 2153-2170.

Fouquart, Y., B. Bonnel and V. Ramaswamy: Intercomparing shortwave radiation codes for climate studies. *J. Geophy. Res.*, **96**, 8955-8968.

Goody, R. M., R. West, L. Chen, and D. Crisp, 1989: The correlated-k method for radiation calculation in nonhomogeneous atmospheres. *J. Quant. Spectrosc. Radiat. Transfer.*, **42**, 539-550.

Joseph, J. H., W. J. Wiscombe, and J. A. Weinman, 1976: The delta-Eddington approximation for radiative flux transfer. *J. Atmos. Sci.,* **33**, 2452-2459.

Kandel, R., and co-authors, 1998: The ScaRab earth radiation budget dataset. *Bull. Amer. Met. Soc.*, **79**, 765-784.

Lacis, A., and V. Oinas, 1991: A description of the correlated k-distribution method for modeling nongray gaseous absorption, thermal emission, and multiple scattering in vertically inhomogeneous atmospheres. *J. Geophy. Res.*, **96**, 9027-9063.

Rothman, L. S., R. R. Gamache, A. Barbe, A. Goldman, L. R. Brown, R. A. Toth, H. M. Pickett, R. L. Poynter, J.-M. Flaud, C. Camy-Peyret, A. Barbe, N. Husson, C. P. Rinsland, and M. A. Smith, 1987: The HITRAN data base: 1986 edition. *Appl. Opt.*, **26**, 4058-4097.

Stamnes, K., S.-C. Tsay, W. Wiscombe, and K. Jayaweera, 1988: Numerically stable algorithm for discrete-ordinate-method radiative transfer in multiple scattering and emitting layered media. *Appl. Opt.*, **27**, 2502-2509.

World Meteorological Organization, 1985. *Atmospheric Ozone, Global Ozone Research and Monitoring Project*. Vol. **I**, Report No. **16**, 392 pp.

Table 1. Gaseous absorption and Rayleigh scattering in the broadband radiation parameterizations and the equations used for transmittance and flux calculations.

Band	Spectral Range (cm^{-1})	Absorber/ Scatterer	Equation
1	(44440-57140)	O_3 Rayleigh	16 --
2	(40820-44440 35700-38460)	O_3 Rayleigh	16 --
3	(38460-40820)	O_3 Rayleigh	16 --
4	(33900-35700)	O_3 Rayleigh	16 --
5	(33330-33900)	O_3 Rayleigh	16 --
6	(31250-33330)	O_3 Rayleigh	16 --
7	(25000-31250)	O_3 Rayleigh	16 --
8	(14280-25000)	O_3 Rayleigh	16 --
9	(8200-14280)	H_2O	13, 15
10	(4400-8200)	H_2O	13, 15
11	(1000-4400)	H_2O	13, 15
Total Spectrum		O_2	18
Total Spectrum		CO_2	21

Table 2. Absorption and scattering in minor bands parameterized in this study.

Band	Spectral Range (cm^{-1})	Absorber/ Scatterer	Equation	Remark
8	(14280-25000)	H_2O	16	
9	(8200-14280)	O_3 Rayleigh	16 --	O_3 absorption folded into Band 8
10	(4400-8200)	Rayleigh	--	
Total Spectrum		O_2	18	New parameterization to include minor absorption bands
Total Spectrum		CO_2	21	New parameterization to include minor absorption bands

Table 3. Effects of minor absorption and scattering on the solar heating of the surface from detailed high spectral-resolution calculations and parameterizations. Fluxes are computed for a typical mid-latitude summer atmosphere. The solar zenith angle and the surface albedo are set to 60° and zero, respectively. The units of heating are W m^{-2}.

	Detailed Calculations	Parameterization
Water vapor in PAR	-2.53	-2.42
Ozone in near infrared	-0.56	-0.54
Oxygen in near infrared	-4.29	-4.18
CO_2 in middle infrared *	-3.30	-3.60
Rayleigh in near infrared *	-3.12	-2.82

* Overlapping with water vapor absorption is included.

FIGURE CAPTIONS

Figure 1. Spectral distribution of the ozone transmission function of the entire atmospheric column in the vertical direction averaged over 10 cm^{-1}.

Figure 2. Same as Fig. 1 except for the water vapor transmission function.

Figure 3. Same as Fig. 1 except for the O_2 transmission function.

Figure 4. Same as Fig. 1 except for the CO_2 transmission function.

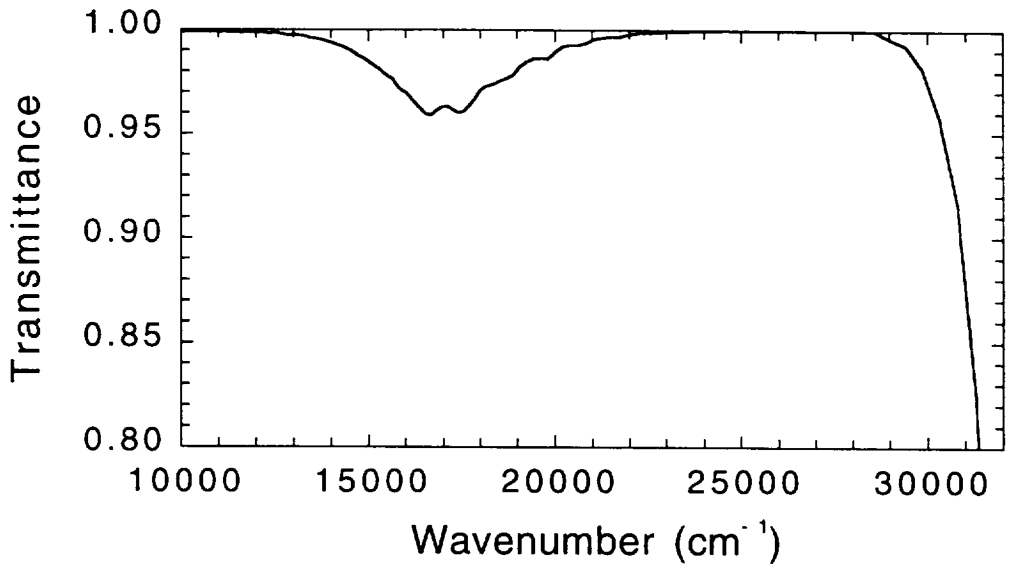
1.00
0.95
0.90
0.85
0.80
Transmittance
10000
15000
20000
25000
30000
Wavenumber (cm⁻¹)

Fig. 1 (Chou)

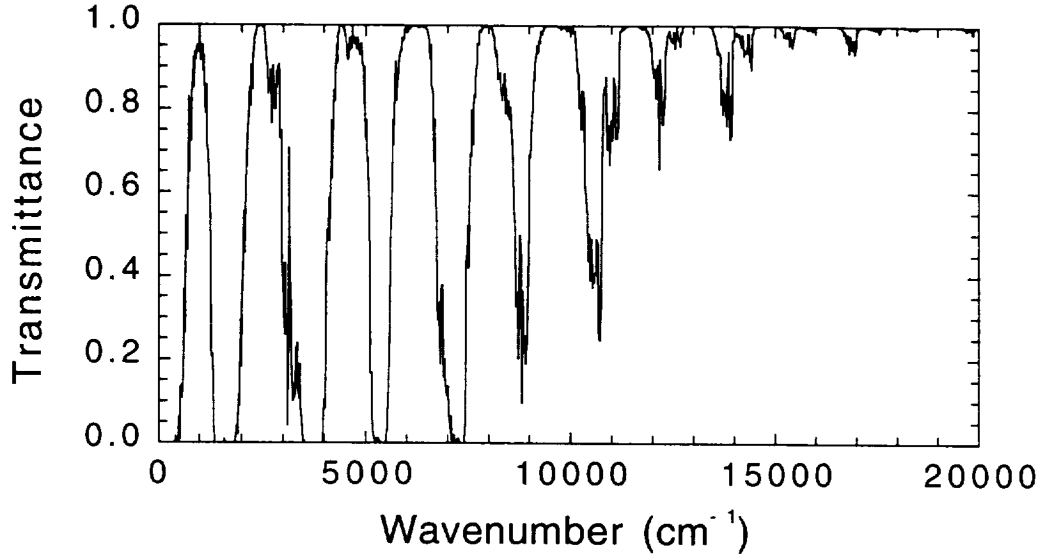
1.0
0.8
0.6
0.4
0.2
0.0
Transmittance
0
5000
10000
15000
20000
Wavenumber (cm⁻¹)

Fig. 2 (Chou)

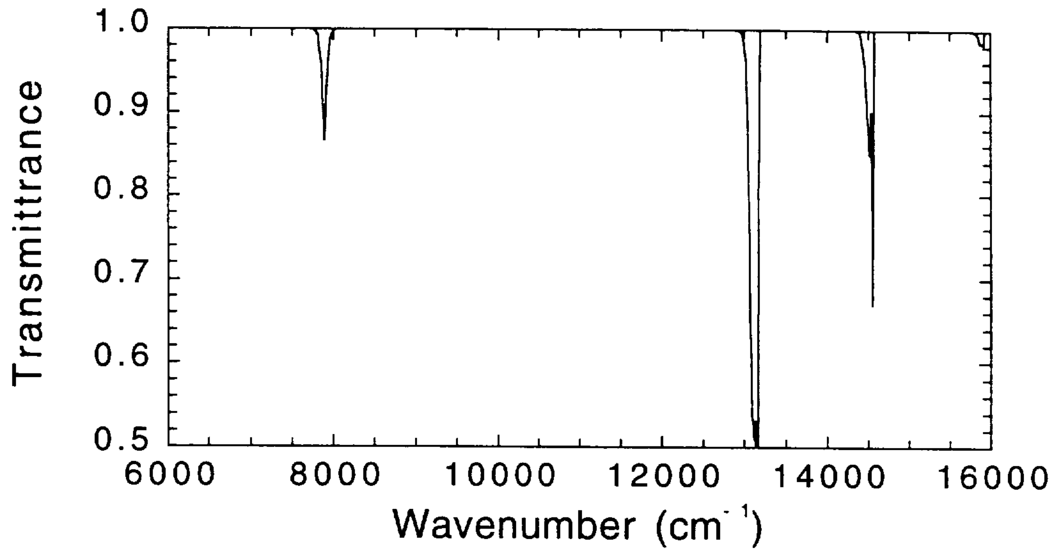
1.0
0.9
0.8
0.7
0.6
0.5
Transmittrance
6000
8000
10000
12000
14000
16000
Wavenumber (cm⁻¹)

Fig. 3 (Chou)

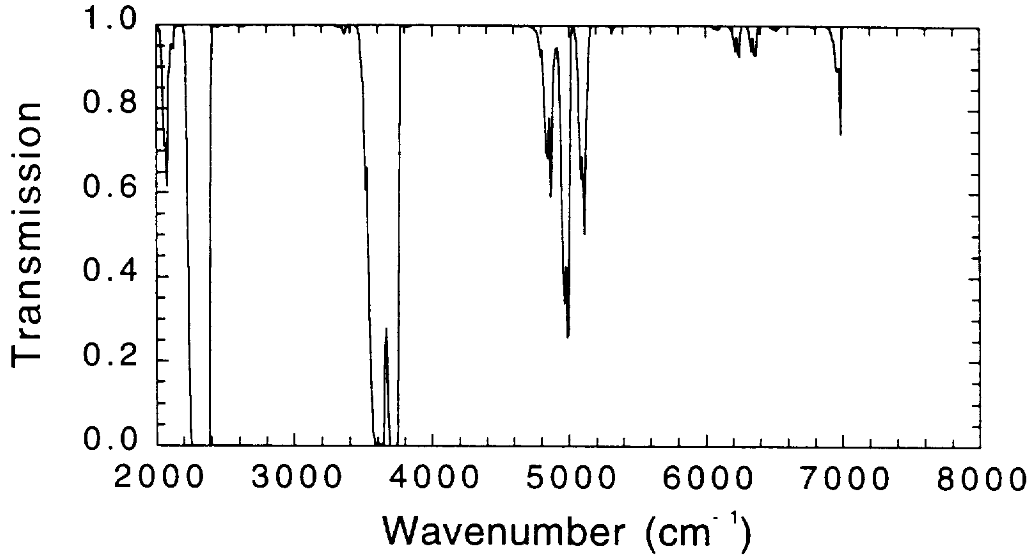
1.0
0.8
0.6
0.4
0.2
0.0
Transmission
2000
3000
4000
5000
6000
7000
8000
Wavenumber (cm⁻¹)

Fig. 4 (Chou)